ELSEVIER

International Journal of Mass Spectrometry 185/186/187 (1999) 517–532

International Journal of Mass Spectrometry

Dissociation rates of energy-selected benzene cations: comparison of experimental results from ion cyclotron resonance and cylindrical ion trap time-of-flight mass spectrometry

Th.L. Grebner[a], H.J. Neusser[b,*]

[a]*Laboratorium für Organische Chemie, ETH-Zürich, Universitätsstr. 16, CH-8092 Zürich, Switzerland*
[b]*Institut für Physikalische und Theoretische Chemie, Technische Universität München, Lichtenbergstrasse 4, D-85748 Garching, Germany*

Received 9 June 1998; accepted 27 August 1998

Abstract

Millisecond decay rates of the perdeuterio benzene cation ($C_6D_6^+$) are measured in two different ion storage equipments. Resonance-enhanced two photon ionization with a single laser beam leads to the production of the perdeuterio benzene cations without internal energy. By absorption of a third photon from the same laser or a second laser beam the ions are excited to internal energies of 4.64 eV and the decay rate is measured by the time dependent appearance of the $C_6D_5^+$ and $C_6D_4^+$ fragment within the electro-magnetic trap (Penning trap) of an ion cyclotron resonance (ICR) mass spectrometer and an electrodynamical ion trap (Paul trap) incorporated in a reflectron time-of-flight mass spectrometer. After correction for infrared relaxation we obtain a unimolecular decay rate constant of 1.15×10^3 s^{-1}. We perform RRKM calculations for this experimental result and for previous values achieved from decay rate measurements in a reflectron mass spectrometer. They are in good agreement with the experimental dependence of decay rate constants for benzene ($C_6H_6^+$) and perdeuterio benzene cations ($C_6D_6^+$) over a wide range of decay rate constants between 10^3 and 2×10^6 s^{-1}. (Int J Mass Spectrom 185/186/187 (1999) 517–532) © 1999 Elsevier Science B.V.

Keywords: Benzene cation dissociation; Energy selection; Fourier transform ion cyclotron resonance; Paul trap

1. Introduction

The benzene cation has been a prototype system for the investigation of unimolecular decay mechanisms of a polyatomic system with many degrees of freedom. Four different decay channels were observed in the range of 4.5–6 eV internal energy, two of them leading to hydrogen fragments (H, H_2; H-loss channels) and the other two to carbon containing neutral fragments (C_2H_2, C_3H_3; C-loss channels). Basic information on the decay mechanism was expected from measurements of the decay rates.

Decay rate measurements were first performed for $C_6H_5^+$ (H-loss), $C_4H_4^+$ (C-loss) formation with the charge exchange technique [1]. As both decay rates were found to be different, this result was interpreted as an example for noncompeting decay channels and a nonstatistical decay from isolated states. This was corroborated by Rosenstock et al. [2]. However, from branching ratio measurements of different C_6H_6 iso-

* Corresponding author.

Dedicated to Professor Michael T. Bowers on the occasion of his 60th birthday.

PII S1387-3806(98)14157-X

mers with the photoion photoelectron coincidence (PIPECO) technique Baer et al. [3] concluded that the channels are competing. In recent work we have shown that the decay rate dependence on the internal energy [i.e. the $k(E)$ dependence] can be very well described by a statistical Rice, Ramsperger, Kassel, Marcus (RRKM) decay model. Our experiments led to the excitation and production of benzene cations at a defined internal energy level above the dissociation threshold. This was possible in a resonance-enhanced two-photon excitation process of the neutral benzene molecule leading to benzene cations with practically no internal (vibrational) energy. The vibrationally cold benzene cations were excited to various internal energies after the absorption of an additional photon from another delayed laser pulse the wavelength of which was changed in a controlled manner. The so excited final electronic state was the $C(^2A_{2u})$ or $D(^2E_{1u})$ state of the ion. The excitation leads to a decay of $C_6H_6^+$ which was detected in a reflectron mass spectrometer as it occurs during the flight time of the ions in its acceleration and drift region [4]. Because of the high mass resolution of the reflectron time-of-flight (TOF) mass spectrometer the production rates of all C-loss and H-loss channels have been measured separately for various defined internal energies between 4.5 and 5.6 eV [5]. We were able to show that C-loss and H-loss decay channels are competing and originate from the same electronic state which, most likely, is the highly vibrationally excited electronic ground state $X(^2E_{1g})$ of the ion. From this result we concluded that after the electronic excitation of the ion a fast nonradiative electronic excitation process (internal conversion, IC) takes place followed by a fast intramolecular redistribution (IVR) process. This is in line with recent theoretical results predicting an ultrafast vibronic relaxation process because of the conical intersection of the exited state potential surfaces [6] and the experimental finding of [7] that no fluorescence from the electronically excited benzene ion could be detected.

The individual decay rate constants $k(E)$ were directly obtained from the total decay rate constant and the branching ratio of the four channels. In addition decay rate measurements for various isotopes yielded a broad data basis: We were able to fit all isotopic data with a single set of vibrational frequencies and their isotopic changes. This demonstrates that the RRKM parameters we found are very reliable. Using RRKM theory we were able to extrapolate the measured $k(E)$ curves to lower energies and to determine accurate dissociation thresholds for each of the four decay channels. While the two H-loss channels dominate in the low excess energy range, a channel switch occurs around 5.3 eV internal energy and the C-loss channels are found to be the most efficient ones at higher energies.

To check the validity of the RRKM theory further, it is interesting to extend the decay rate measurements to lower internal energies and slower dissociation rates. Recently, Klippenstein et al. performed new calculations with variational RRKM theory leading to a refined description of the transition state for the elimination of an H atom [8]. The theoretical results were in satisfactory agreement with the above mentioned $k(E)$ curves and with new experiments of these authors in the low excess energy range. Their experiments include decay rate measurements of the laser-induced dissociation of benzene cations in an ion cyclotron resonance trap. The lowest internal energy of 4.48 eV was smaller than in our recent experiments, this leading to a smaller decay rate constant of $1.32 \times 10^3\ s^{-1}$ which could be measured because of the long storage time of the ICR instrument but was not accessible in our reflectron TOF because of the short flight times. Although the agreement of their decay rate data with theory was reasonable there is some question as to the effect of the width of the energy distribution on the measured decay rates. Klippenstein et al. used ions with a thermal energy distribution leading to an internal energy width of about 0.13 eV in case of the benzene cation.

In the present work we would like to report on slow decay rate measurements performed in an ICR instrument under collision-free conditions and starting from a nonthermal energy distribution of laser-produced and -excited benzene cations. The width of this energy distribution is investigated in detail using photoelectron time-of-flight spectroscopy (PES) and the technique of mass analyzed threshold ionization

(MATI). It is found to be different and narrower than for thermalized cations. The decay rates measured with the ICR setup are then compared with similar experiments performed in a home-built simple cylindrical ion trap. On the basis of this result we are able to decide whether the low cost version of an ion trap is suitable for decay time investigations in the ms time range. After correction of the measured rates for radiative IR relaxation processes we compare the decay rate results of this work with the recent values of [8] and the predictions of statistical theories.

2. Experimental setups for measuring MS decay times

Measuring small dissociation rate constants requires the possibility of storing the species under investigation in a defined volume. This is necessary because experimental conditions e.g. in a time-of-flight mass spectrometer lead to a fast escape of the dissociating ions from the detection window because of their kinetic energy after acceleration. Two different experimental concepts have been used in this work for this purpose: (i) the electro- and magnetostatic Penning trap installed in a commercially available Fourier transform ion cyclotron resonance mass spectrometer (FTICR-MS) which has gained great importance in time-resolved photodissociation measurements [9] and (ii) a home built electrodynamical cylindrical ion trap incorporated in a time-of-flight mass spectrometer which was also home made. The two experimental setups are described in the following.

2.1. FTICR mass spectrometer

The FTICR-MS used in this work is the CMS 47X ICR Mass Spectrometer manufactured by Spectrospin AG/Switzerland. The Penning trap in this instrument consists of two discs (trapping electrodes) with ~60 mm diameter which are separated by 60 mm. These two electrodes provide the electrostatic trapping potential in the direction along the magnetic field. The magnetic field (4.7 T) points into the direction (z direction) which is perpendicular to the two trapping electrodes. The voltages applied to the trapping electrodes is of the order of 1 V. The space in between the trapping electrodes is surrounded by a tube with 60 mm diameter which is divided into two pairs of opposing sections. One pair of these electrodes is used for excitation of the ions and the other pair is used for recording the electrostatic induction caused by the cycling ions. For more details on the ICR mass spectrometer, see e.g. [10]. The ICR was originally equipped with an differentially pumped external ion source with an electron gun for ionization. Note that the external ion source of the Munich ICR instrument is now considerably modified and extended by a fourth differential pumping stage with the possibility of mounting a variety of different ion sources [11].

In this work we used the original effusive sample inlet consisting of a quartz capillary mounted in the center of the flange which terminates the external ion source. The capillary is centered in respect to the axis of the Penning trap. This is quite important because guiding ions from a region with low magnetic field into the strong field of 4.7 T present inside the trap can only be achieved efficiently for ions very close to the rotational axis of the magnetic field.

The production of perdeuterio benzene cations is achieved by a one-color two-photon ionization scheme via the 6_1^0 "hot band" transition at 37 723 cm^{-1} by focusing the pulsed laser light of a Molectron Corp. DL II dye laser (~50 μJ) pumped by a UV24 Molectron nitrogen laser (~8 mJ pulse energy at 337 nm) close in front of the capillary. The so produced cations are guided into the Penning trap by the ion optics of the CMS 47X. Although a short duration pulsed laser light source (ns) leads to a small bunch of ions which is mapped into the trap by the ion optics with only minor distortion there is also a well defined small cloud of ions present in the trap after ion trapping. The kinetic energy of the trapped ions is about 0.5 eV in the z direction. This kinetic energy leads to a spatial oscillation of the ion cloud along the z axis according to the trapping frequency (in the order of 100 kHz) with an amplitude only slightly smaller than the length of the trap. Because the excitation field is distorted by the trapping electrodes

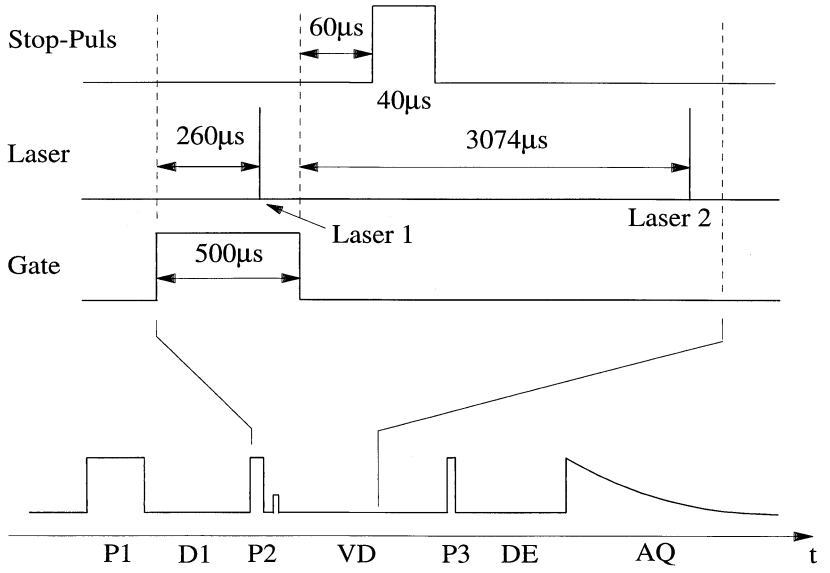

Fig. 1. Timing sequence of the measuring cycle for decay rate measurements with the FTICR mass spectrometer. For a detailed description, see text.

preferentially close to the trapping electrodes the excitation efficiency of an ion depends on its actual position on the *z* axis within the trap because the excitation time is much smaller than the time for one cycle of the trapping motion. Consequently, the detection efficiency in our experiment originally depended on the position, respectively on the phase of the axial trapping motion. Unfortunately, a phase lock between triggering the laser and starting the ion transfer, excitation and acquisition sequence is not possible for the FTICR-MS used.

To avoid a phase dependent detection efficiency a stopping mechanism of the ions has been developed in order to reduce the amplitude of the motion of the ion bunch along the *z* axis. For this purpose the trapping electrode to which the ion cloud heads on when it enters the trap is set to a voltage of 1.4 V for 40 μs in order to decelerate the motion of the ion bunch moving towards this electrode at that moment.

The first two steps of the measuring cycle are *P*1 and *D*1 during which all ions are swept out off the trap in order to clean the trap at the beginning of every measuring cycle (see Fig. 1 for the timing sequence of the experiment). During *P*2 ions can enter the ion trap. This is accomplished by setting electrodes called gate which are mounted close to the trap entrance to proper potentials. The ionizing laser is triggered approximately right in the middle of the period when the gate is open (see upper part of Fig. 1). The delay time between the ionizing laser pulse and the stop pulse is set to 300 μs to account for the transfer time of the ion bunch from the external ionization region into the trap. All trapped ions are now close to the axis of the trap moving with a small cyclotron radius because their kinetic energy in the *r* direction which describes the plane perpendicular to the *z* axis is only in the order of 1 eV. Consequently, they can be irradiated by a centered laser beam with a small diameter pointing into the *z* direction. For the optical excitation of the trapped benzene cations we utilized the fourth harmonic light of a Nd:Yag laser (GCR 3, Spectra Physics) with 3 mJ pulse energy. The absorption of one photon from this laser pulse leads to an excess energy of 4.66 eV. This exciting laser is triggered 3074 μs after the gate is closed. During *P*3 (25 μs) the charged dissociation product ($C_6H_5^+$) is excited to a large cyclotron radius by applying a certain burst of alternating voltage to the pair of excitation electrodes of the ion trap. The FTICR is operated in a mode in which only a single species (the

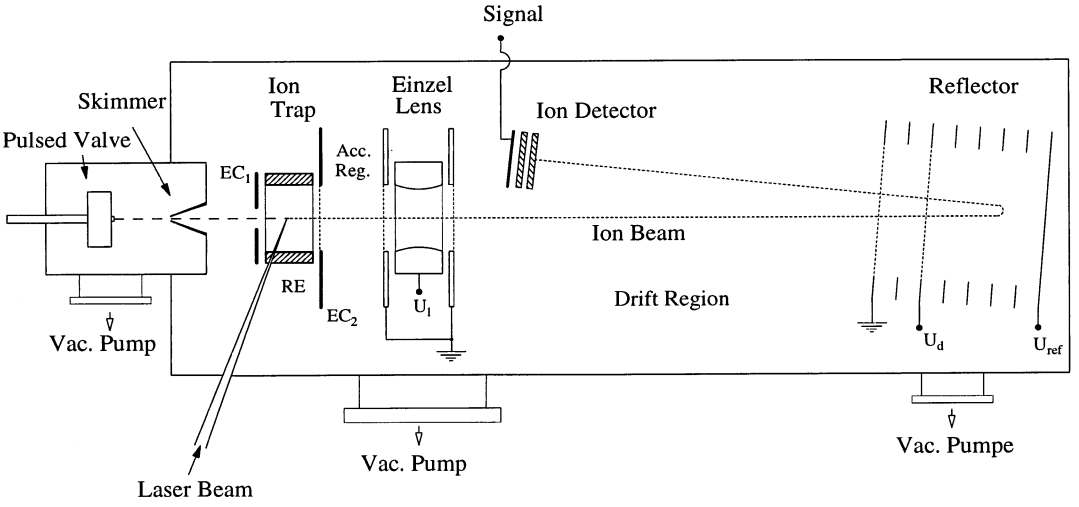

Fig. 2. Schematic drawing of the CIT-RETOF mass spectrometer setup. It consists of two vacuum chambers separated by the skimmer. The first chamber contains the pulsed valve for production of the supersonic molecular beam. In the second chamber the cylindrical ion trap (CIT) with the two end caps (EC_1 and EC_2) and the ring electrode (RE) is installed. The additional ion optics and the ion detector are part of the RETOF mass spectrometer. Ions are produced by one-color two-photon ionization in a laser beam intersecting the CIT perpendicular to the molecular beam.

fragment ion) is excited to a large cyclotron radius. The sequence variable delay (VD) permits the variation of the time delay between optical excitation of the ions by laser 2 and the cyclotron excitation of the dissociation product. The signal produced by the alternating charge influenced in the pair of detection electrodes by the cycling ions is recorded during acquisition (AQ). A subsequent Fourier transformation yields the mass spectrum. The AQ of the ion signal needs about 0.3 s. This means that the repetition rate of the measuring cycle is limited to ca. 3 Hz. For recording the increase of the concentration of the dissociation product ions with increasing trapping time the VD is changed between 50 and 2150 μs with an offset of 3074 μs.

2.2. CIT-RETOF mass spectrometer

The experimental setup of the experiment with the cylindrical ion trap incorporated into a reflecting mass spectrometer (CIT-RETOF) has been described previously [12]. Briefly, the trap consists of a short tube and two thin discs on each side of the tube. In our design (see Fig. 2) the end cap (EC_1) at the entrance side of the molecular beam is a solid disc with a central hole of 3 mm and an outer diameter of 35 mm. The ring electrode (RE) has an inner diameter of 20 mm and is 13.14 mm long. The length/diameter ratio is chosen to 0.707, hence inscribing an hyperbolical ion trap with radius r = 1 cm and $z = \sqrt{0.5} \times r$ [13]. This ratio is achieved by additional isolating nylon spacers between the ring electrode and the end caps. The exit electrode consists of copper mesh with 1/20 of an inch spacing covering the hole (20 mm diameter) in the EC_2 electrode. The laser beam crosses the ring electrode in its center through two holes of 3 mm diameter. EC_2 together with the left electrode of the einzel lens form the acceleration region (Acc. Reg.) of the RETOF mass spectrometer. The CIT is operated in the "total storage mode" with all three electrodes at the same dc voltage (BIAS) and rf voltage applied only to the ring electrode.

Different from the experiment with the FTICR instrument the molecules are cooled in a supersonic jet. The jet is obtained by seeding the vapor of perdeuterio benzene into Ar carrier gas at $\approx$3 bar backing pressure and expanding the mixture into the vacuum through the orifice of a pulsed valve. The

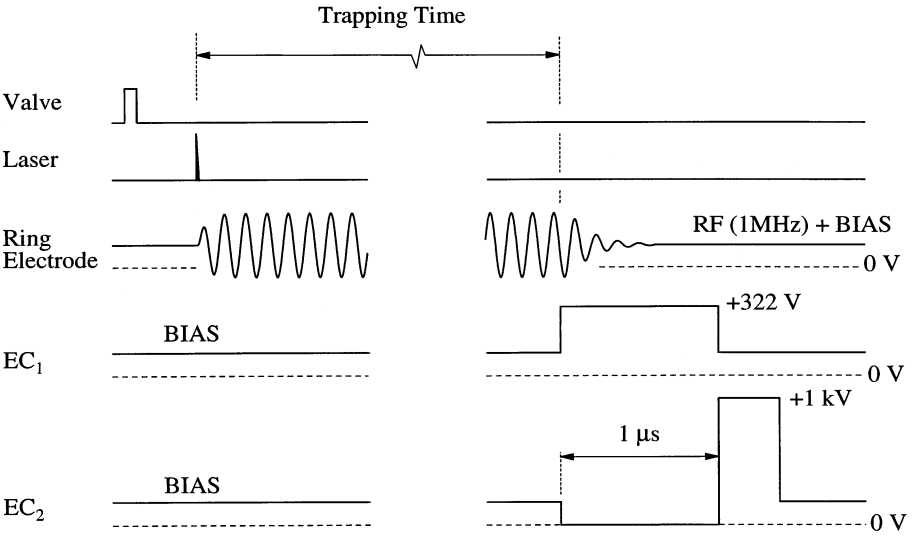

Fig. 3. Timing sequence of the measuring cycle for decay rate measurements with the CIT-RETOF mass spectrometer. For a detailed description, see text.

ionization and excitation of the benzene molecules is achieved by laser light from a single dye lasers with ≈10 ns FWHM light pulses and ≈0.3 cm^{-1} bandwidth (FL 3002; Lambda Physik), which is pumped by an excimer laser (EMG 1003i, 308 nm; Lambda Physik).

The time sequence of the experiment occurs as follows (see Fig. 3): A master trigger (10 Hz, synchronous with the line frequency) triggers the pulsed piezo valve with an opening time of less than 150 μs. At this time the three electrodes of the CIT are connected to a positive voltage (BIAS = +93 V) and no rf voltage is applied to the ring electrode. After an appropriate time delay which is sufficient for the molecules to travel through the skimmer into the CIT the laser is triggered. When the rf voltage crosses zero after the occurrence of the laser pulse the rf voltage is applied to the ring electrode by a synchronization circuit. Because the frequency of the rf is ~1 MHz there is a jitter of 1 μs between ion creation by the laser pulse and the application of the rf voltage. This synchronization procedure was necessary because to transfer the ions out of the trap was more stable if this phase looked switching on of the trapping voltage was used instead of having the rf voltage on continuously during ion formation. The rf voltage (sine wave, 72 V amplitude, 985.5 kHz) is present at the ring electrode during the entire time of trapping, with the BIAS voltage connected to all three electrodes. To extract the ions from the CIT a second synchronization process is started by the delay circuit which controls the trapping time. The trigger for the end of the trapping time activates the synchronization device which switches the rf voltage off at a fixed phase of the rf voltage. About 200 ns later the end cap EC_1 is set to a higher positive voltage (322 V) and simultaneously EC_2 is pulled down from BIAS to ground (0 V). Now the ions travel to the acceleration region, which is 20 mm long. This takes about 1 μs. In the acceleration region the ions are accelerated again by applying +1 kV to EC_2. With the einzel lens (U_1 = +63 V) the ion paths are slightly focused. The length of the field-free drift region is 60 cm. After reflection in the two sector reflector [14,15] (25 mm and 182 mm) (deceleration voltage U_d = 520 V, reflector voltage U_{ref} = 1 kV) the ions hit the double layer microchannel plate (MCP) detector (see Fig. 2). The average background pressure in the main vacuum chamber of the CIT-RETOF is between 7×10^{-8} and 1×10^{-7} mbar. From the short duration of the gas pulse (600 μs) of the pulsed valve, the "open" design of the CIT and the low repetition rate of the experi-

ment the pressure inside the trap is expected to be similar. Time-of-flight spectra are monitored with a digital oscilloscope (LeCroy 9350A). The intensity of stable ions or charged dissociation products are recorded mass selectively as a function of trapping time with a gated integrator/microcomputer set up.

3. Production of state selected-ions

The most promising method for production of internal energy selected ions is photoionization with vacuum-UV photons of defined energy. However, the absorption of monochromatic photons does not automatically lead to ions with defined internal energy because the photoelectrons carry away a variable amount of energy and leave behind ions with broad internal energy distribution. If ions are monitored in coincidence with electrons of defined kinetic energy (photoion-photoelectron coincidence technique) the internal energy of the ions is also defined. In recent experiments a resolution of better than 20 meV has been achieved with this method [16].

An alternative method for the production of internal energy selected ions is resonance-enhanced multiphoton ionization (REMPI). In this method efficient ionization is achieved by stepwise multi photon ionization via a resonant intermediate state [17–19]. This resonance enhancement of the multi photon ionization process does not only lead to a drastic increase of the ionization yield but also results in a high selectivity of the ion production. The intermediate state controls the ionization process and this often leads to the preparation of an ensemble of dissociating molecules with closely defined energy.

For practical reasons, because only a limited number of tunable lasers is available we selected a special transition leading to a moderate excess energy in the benzene cation when a single laser is used for excitation: This is the 6_0^1 hot band transition at a frequency of 37 723 cm^{-1} in C_6D_6. After the absorption of two photons of this energy via the 6^0 intermediate state the excess energy above the ionization energy (IE) is $\Delta E = 178$ meV. The excess energy can distribute to either the kinetic energy of the electron or the internal energy of the ion. This process is governed mainly by the Franck Condon factor for the transition from the intermediate state to the vibrational states of the ion within the excess energy range. In order to check whether the ions are produced in a single vibrational state, an analysis of the photoelectron energy must be performed. For the energy analysis of low energy electrons (<500 meV) time-of-flight photoelectron analyzers are advantageous [20,21]. A photoelectron spectrum of C_6D_6 achieved by one-color two-photon ionization via the 6_1^0 transition is shown in Fig. 4. The energy scale of the photoelectron spectra directly represents the ion internal energy. It is seen that for the chosen intermediate state the ionic 0^0 band carries about 90% of the intensity of the $X(^2E_{1g})$ ground state spectrum. However, there appear three much weaker peaks to higher excess energy corresponding to the 16^1, 6^1 (1/2), and 1^1 vibrational states. As the detection probability for electrons is nearly constant down to a kinetic energy of 50 meV most likely the peak intensities in Fig. 4 reflect the population probability of the individual vibrational states. Franck Condon factors favor the population of the vibrationless 0^0 state though the second photon energy is sufficient to produce the 1^1 state at 115 meV (925 cm^{-1}).

For comparison, in Fig. 5 we present a vibrational spectrum of the $C_6D_6^+$ cation displaying a higher resolution than the time-of-flight photoelectron spectrum. It was measured with the technique of mass analyzed pulsed field threshold ionization (MATI) [22,23].

Briefly, MATI spectroscopy is based on the pulsed field ionization of molecules into high ($n > 40$) long-lived Rydberg states which exist nearby an ionization threshold of the molecular cation. The neutral long-lived Rydberg molecules are separated from the ions produced simultaneously in a prompt ionization process by a weak electric field (0.3 V/cm) which accelerates or decelerates the ions but does not affect the Rydberg molecules except ionizing those Rydberg molecules which are very close ($n > 250$) to the ionization threshold. After the spatial separation of the Rydberg molecules from the prompt ions the surviving Rydberg molecules are converted into “threshold ions” by a delayed pulsed stronger electric

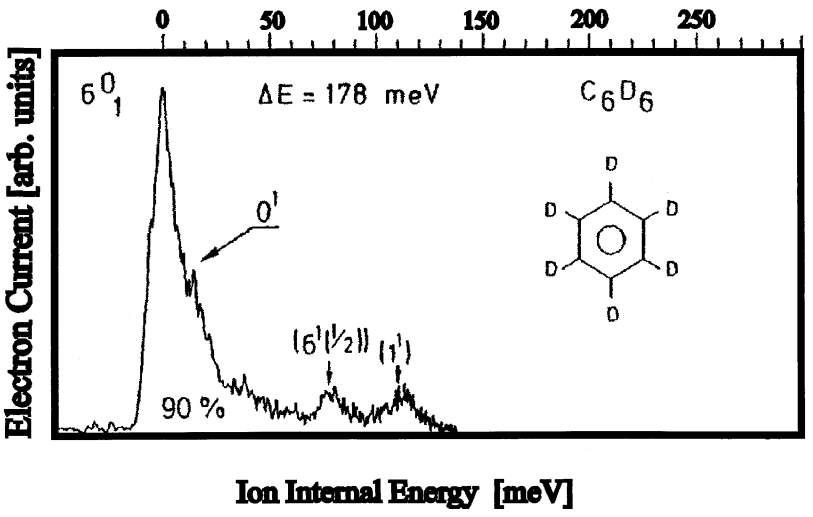

Fig. 4. Time-of-flight photoelectron spectrum of perdeuterio benzene obtained by resonantly-enhanced two-photon ionization via the 6^0_1 hot band transition. The electron takes away most of the excess energy (ΔE) leaving the benzene cation preferentially in its vibrationless ground state [33].

field (500 V/cm). The threshold ions contain a very well defined amount of internal energy and are detected in a mass selective way.

In the spectra of Fig. 5, clearly several vibrational peaks are resolved which have been assigned. The first laser frequency was fixed to the 6^0_1 hot band (top) or the 6^1_0 cold band (bottom) transitions and the second photon is from a second tunable laser whose frequency was scanned from below the first ionization threshold up to ca. 1200 cm^{-1} internal energy. Whenever high Rydberg states converging to the various ionic vibrational states are excited a threshold ion signal is observed marking the energetic position of the vibrational states of the ion after field correction with an accuracy of ca. ± 2 cm^{-1}. In the lower spectrum (via 6^1_0) the 6^1 state acts as an intermediate state. Because of suitable Franck Condon factors the strongest peak in the threshold ion spectrum corresponds to the same vibrational state, i.e. the 6^1 state, in the ion. The high resolution of the MATI technique leads to the observation of a splitting of this band because the quadratic Jahn-Teller effect [23,24]. On the other hand, when the vibrationless S_1 state acts as an intermediate state (upper trace), according to the angular momentum selection rules, in this case only Jahn-Teller states with a total angular momentum of 1/2 should be present in the spectrum and the 0^0 state of the ion produces the strong peak in the threshold ion spectrum. In this spectrum the $6^1(\pm 3/2)$ band has completely vanished. Instead, the much weaker 4^1 band becomes visible at this position.

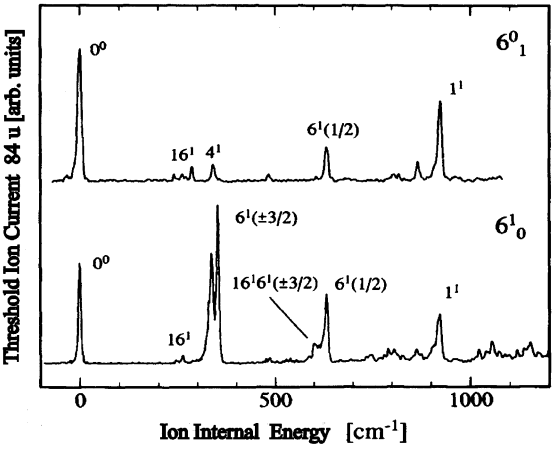

Fig. 5. Mass analyzed threshold ionization (MATI) spectra of the cationic ground state of perdeuterio benzene obtained by resonantly-enhanced two-photon two-color excitation. The upper spectrum is measured with the first laser frequency fixed to the 6^0_1 hot band $S_1 \leftarrow S_0$ transition and the lower trace is obtained by pumping via the 6^1_0 transition [34].

From a comparison of Fig. 4 and Fig. 5 it is seen that the peaks in the photoelectron spectrum basically agree with the vibrational peaks present in the MATI spectrum and a clear assignment of the lower resolution photoelectron spectrum becomes possible. In conclusion we find from the TOF photoelectron spectrum which represents the experimental situation of the decay rate measurements that for the one-laser two-photon excitation resonantly enhanced via the 6^0 state the preferential production of ion in the vibrational ground state takes place. Thus the ions produced in this way contain, if at all, only a small amount of vibrational energy. After we have discussed the vibrational energy contents we have to briefly consider the rotational energy distribution. In the CIT experiments a supersonic jet expansion is used leading to a rotational temperature of about 2 K and thus to a negligible energy contents. On the other hand in the ICR experiment benzene cations are produced in an effusive molecular beam with thermal temperature. In principal, a selection of rotational intermediate states leads to largely defined rotational states of the cation. This was demonstrated in our previous experiments [25]. However for the low resolution laser used in the present experiments with the ICR mass spectrometer practically no selection can be achieved and we have to assume a contribution of 3 kT/2 to the internal energy from rotation. As shown in our previous work [25,26] this energy is available for dissociation because a rapid *K*-mixing process and in addition effects of the state density are even more important. Though, the effects on the decay rate are expected to be less than 20% in the populated range of rotational quantum numbers for the investigated internal energies. In summary, resonance enhanced two photon ionization via the vibrationless intermediate state leads to ions which contain, if at all, a small amount of internal energy. This energy is by far not sufficient to induce a dissociation of the ion. The state selected ions have to be further excited by an additional photon absorption. A second laser of variable photon energy is used to excite the cations to different energy levels above their dissociation threshold. The final electronic state is the C ($^2A_{2u}$) or D ($^2E_{1u}$) state of the ion. Excitation leads to a slow metastable decay of the $C_6D_6^+$ cation which is detected in the FTICR or in the reflectron mass spectrometer coupled to the cylindrical ion trap (CIT-RETOF).

4. Results and discussion

4.1. FTICR-MS

For low internal energies the benzene cation preferentially decays by ejection of a D atom or a D_2 molecule (H- or D-loss channels) [5]. First, we measured the increase of the $C_6D_5^+$ fragment ion density as a function of time after laser excitation. In Fig. 6 the increase of the $C_6D_5^+$ ion intensity in the FTICR mass spectrometer after excitation of the stored perdeuterio benzene cations with laser light of $h\nu = 4.661$ eV is shown. From the fit of a single exponential curve to the appearance of the $C_6D_5^+$ daughter ions a dissociation rate constant k^*_{tot} of 1.5×10^3 s^{-1} is obtained. As pointed out above, the four different decay channels are competing and the experimentally measured rate constant k_{tot} is the sum of all four individual decay rates

$$k_{tot} = k_D + k_{D_2} + k_{C_2D_2} + k_{C_3D_3}$$

if no competing decay processes occurs. This means that the total decay rate of the benzene cation can be measured by monitoring the appearance of only one of the daughter products. The main contribution here is from the D-loss channels (k_D, k_{D_2}) for the chosen excitation energy. Because the time for electric excitation of the dissociation product is short compared to the decay time of $C_6D_6^+$ there is no need for a deconvolution of the appearing fragment ion signal from the instrumental function of the FTICR.

4.2. CIT-RETOF mass spectrometer

In the experiment utilizing the CIT-RETOF mass spectrometer ionization of C_6D_6 and excitation of the benzene cation was performed with three photons of the same color. The first and second absorbed photon excites and ionizes the perdeuterio benzene via the 6_1^0 hot band transition. The absorption of the third photon

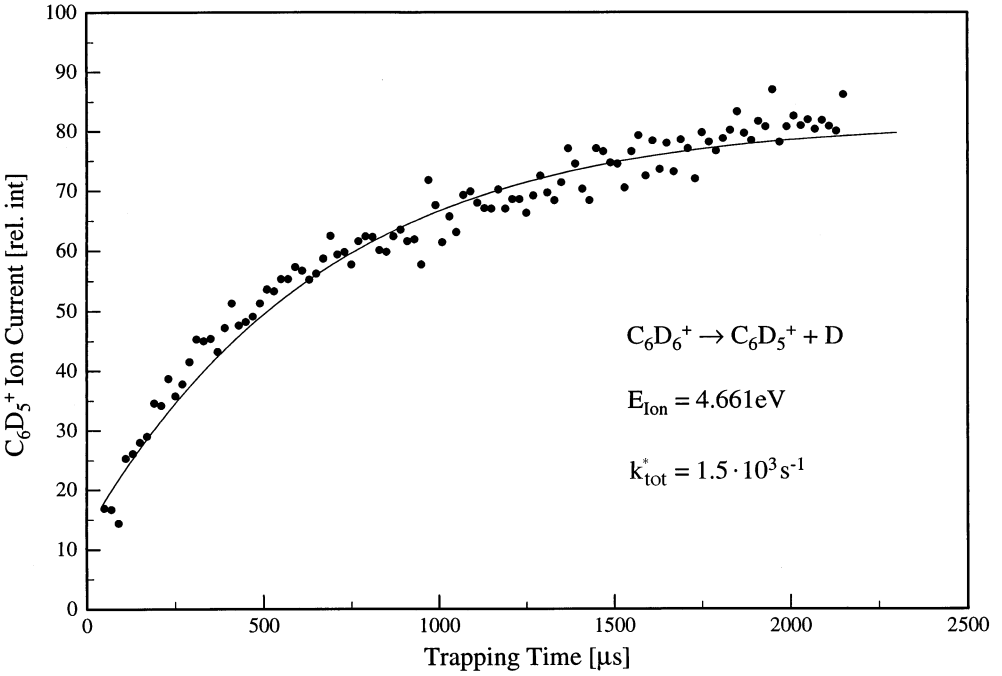

Fig. 6. Signal of the charged dissociation product $C_6D_5^+$ with increasing trapping time after three-photon excitation described in the text. The experimental points in the FTICR mass spectrometer experiment are fitted with a single exponential curve (solid line) yielding a time constant of 1.5×10^3 s^{-1}.

in the cation leads to an ion internal energy of 4.67 eV. In order to avoid absorption of additional photons in the cation which would be followed by a fast decay the laser pulse intensity has to be adjusted carefully. The D-loss (Fig. 7) and D_2-loss (Fig. 8) channels were recorded simultaneously and with a 50 μs stepwise increase of the trapping time from 100 μs up to 4.5 ms. The two other (C-loss) dissociation channels could not be measured because at an ion internal energy of 4.67 eV the loss of a single D atom by far dominates with its large branching ratio. Consequently, the rise of the $C_6D_5^+$ signal with increasing trapping time (Fig. 7) shows less fluctuations than the $C_6D_4^+$ signal (Fig. 8) because of its a much better signal-to-noise ratio. The solid line in each picture represents the fit of an exponential curve to the experimental data. In both cases the fitted curves cross zero intensity at time zero showing that no background of instantaneously produced dissociation products $C_6D_5^+$ and $C_6D_4^+$ are present. Each fitted rising curve is normalized in such a manner that it approaches 100% for $t \rightarrow \infty$. The fitted rate constants k^*_{tot} are 1.51×10^3 s^{-1} for $C_6D_5^+$ and 1.48×10^3 s^{-1} for $C_6D_4^+$, respectively. The measured rate constants k^*_{tot} differs from the rate constant k_{tot} introduced above because of the influence of competing decay processes (see below). These two values are identical within the experimental accuracy and in line with the behavior expected for competing channels. This measured rate constant is also in line with the value obtained in the experiment with the FTICR mass spectrometer. This clearly shows that decay kinetics of larger polyatomic molecules can be measured with a relatively "simple" device especially compared to the FTICR-MS.

4.3. Influence of competing decay processes

4.3.1. Collisions

For the small rate constants measured in this work we have to check whether competing decay channels are active. First we want to consider the possible influence of collisions on the dissociation process. In the ICR trap the pressure was as low as 8.0×10^{-9}

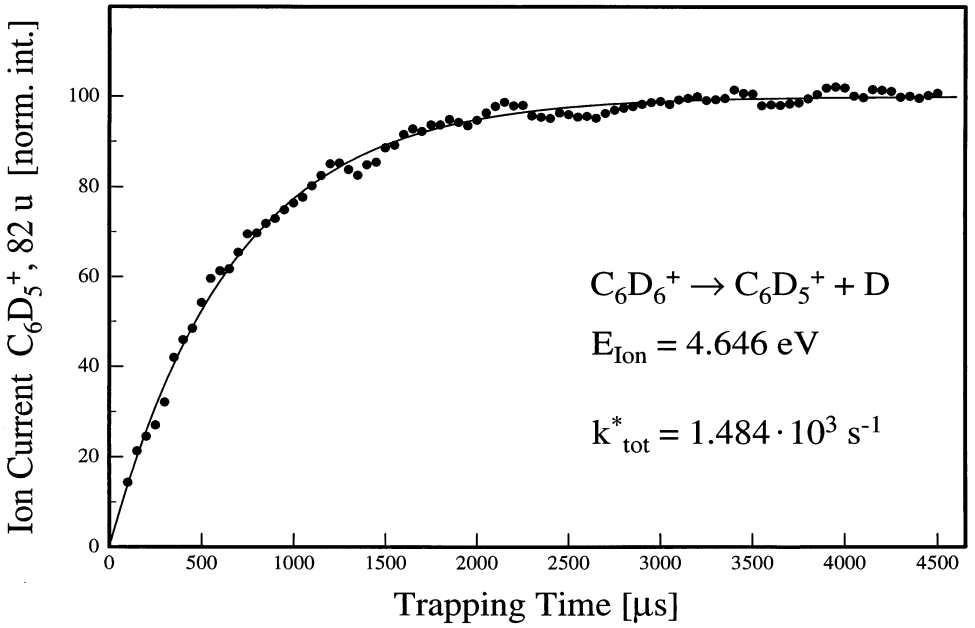

Fig. 7. Signal of the charged dissociation product $C_6D_5^+$ with increasing trapping time after three-photon excitation described in the text. The experimental points in the CIT-RETOF mass spectrometer experiment are fitted with a single exponential curve (solid line) yielding a time constant of 1.48×10^3 s^{-1}.

mbar during the experiment. Furthermore, the number of trapped $C_6D_6^+$ ions is only in the order of 10^4. From these experimental conditions we exclude any influence of collisions on the measured rate in the experiment with the FTICR mass spectrometer. In the experiment utilizing the CIT-RETOF mass spectrometer the average pressure inside the drift chamber (see Fig. 2) is around 1×10^{-7} mbar. The pressure inside the trap is assumed to be almost the same as in drift chamber. We used a piezo-driven valve with short opening time of ca. 150 μs leading to only a small gas load. In order to avoid the absorption of two or more photons by the cation the intensity of the laser pulse (2 mm beam diameter) is kept at a small level leading also to a small number of trapped ions so that an influence of collisions can be virtually excluded.

4.3.2. Additional internal energy components

In the photoelectron spectrum of Fig. 4 two small peaks at higher internal ion energies of 80 and 115 meV are present. The question arises how strong they contribute to the appearance curves in Figs. 6–8. This can be seen from the $k(E)$ curve in our previous work [26] and Fig. 9 of this work. An increase of the internal energy from 4.67–4.78 eV by ca. 100 meV increases the decay rate by nearly a factor of three in the low excess energy range around 4.6 eV. This would lead to a biexponential decay curve with a fast component. Neither in Fig. 6 nor in Figs. 7 and 8 are indications for a biexponential decay observed within the experimental accuracy. Thus we may conclude that no essential contribution to the ion decay exists arising from ions with a larger internal energy, and the measured decay rate represents the decay rate of ions with an internal energy identical to the energy of the third photon with reasonable accuracy.

4.3.3. Infrared relaxation

Hot ions lose their internal energy by emission of infrared photons (IR relaxation). For the small rate constants with a decay time in the ms range measured here the infrared relaxation is an important factor and has to be considered [27]. IR relaxation is taken into account by adding the radiative rate k_{rad} for the

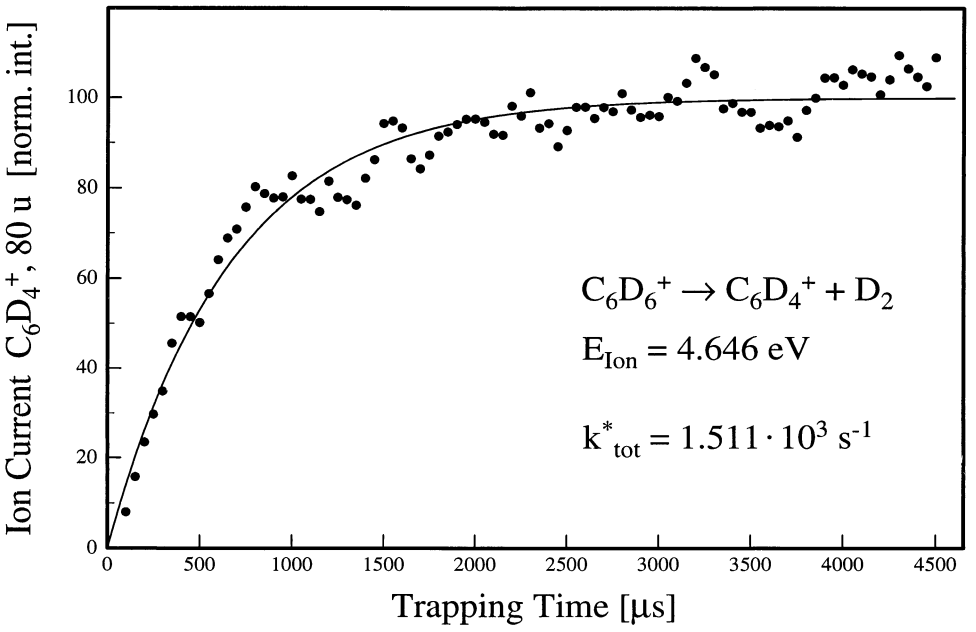

Fig. 8. Signal of the charged dissociation product $C_6D_4^+$ with increasing trapping time after three-photon excitation described in the text. The experimental points in the CIT-RETOF mass spectrometer experiment are fitted with a single exponential curve (solid line) yielding a time constant of 1.51×10^3 s^{-1}.

calculation of the experimentally observed rate constant k^*_{tot}

$$k^*_{tot} = k_{tot} + k_{rad}$$

Consequently, the fitted curve represents the function describing the increase of the dissociation product D^+ with increasing trapping time t plus the influence of the IR emission leading to an additional loss of parent ions from the excited level for dissociation

$$D^+(t) = D^+_\infty(1 - e^{k^*_{tot}t})$$

D^+_∞ is the number of dissociation products reached at a time which is very long compared to the decay time. Here it has been assumed that after emission of a single IR photon the remaining internal energy of the benzene cation is not sufficient for a decay in the ms time window of the experiment and represents a loss channel. For experimental conditions with no dissociation product ions present at the beginning of the trapping time, e.g. for the absence of a fast decay caused by the absorption of two photons in the cation, the fitted curve intersect the time scale at $t = 0$. This is not completely fulfilled in the experiments with the FTICR mass spectrometer but is valid in the experiment with the CIT-RETOF mass spectrometer. The reason for a small background of fragment ions is the high intensity of the second laser (fourth harmonic of Nd:YAG fundamental frequency) leading to the absorption of two photons which excite the perdeuterio benzene cation to an excess energy of ca. 9 eV. This excess energy leads to a very fast dissociation on the sub ns time scale.

In order to correct the experimentally obtained dissociation rates for the influence of the IR emission results obtained by Dunbar and co-workers are used [27,28]. They estimated a value of 700 s^{-1} for the radiative rate k_{rad} at an internal energy around 4.5 eV in $C_6H_6^+$. For the perdeuterio benzene cation k_{rad} is expected to be smaller by a factor of two [29]. A smaller radiative rate for the perdeuterio benzene cation was also observed in its complex with Al [30]. For this reason we take $k_{rad} = 350$ s^{-1} for the radiative rate of $C_6D_6^+$ at an internal energy of 4.64 eV. If we apply this result to the dissociation rates

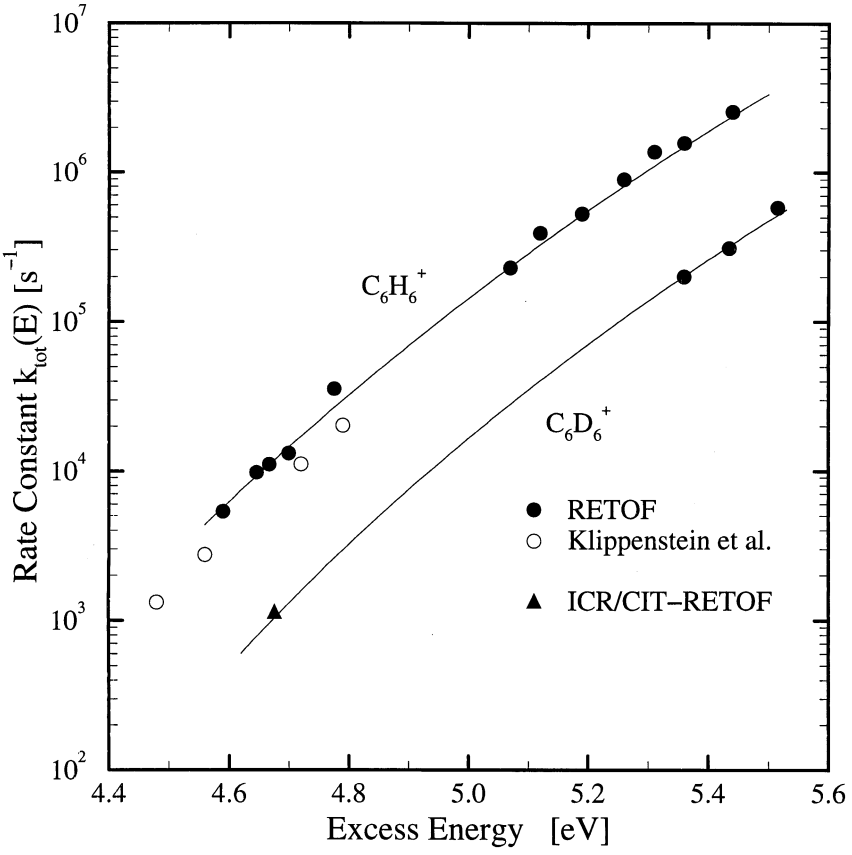

Fig. 9. Dissociation rate constants $k_{tot}(E)$ of benzene and perdeuterio benzene obtained with different techniques: values marked by filled circles were measured in a time-of-flight mass spectrometer [5], values marked by open circles were measured in an FTICR mass spectrometer [8] and the value marked by the filled triangle is measured in the CIT-RETOF and in a FTICR mass spectrometer described in this work. The solid lines represent the result from RRKM calculations.

measured in the present work we obtain a dissociation rate constant of 1150 s^{-1} at the ion internal energy of 4.64 eV.

4.4. Decay kinetics of the benzene cation

For the dissociation of the benzene cation a number of $k_{tot}(E)$ values for defined internal energies are available. The internal energy ranges from ca. 4.5 eV up to 5.4 eV for benzene and from ca. 4.7 eV up to 5.5 eV for perdeuterio benzene (see Fig. 9).

There exist results from two experiments in this energy range, both on $C_6H_6^+$ cations. In our recent review [26] we presented decay rates measured in a reflectron mass spectrometer. The reflectron mass spectrometer was operated in the complete correction mode. In this case, daughter ions produced by a metastable decay in the reflecting field region are distinguishable from those produced by a metastable decay in the acceleration and the drift region yielding a decay rate constant for an assumed exponential decay. The accessible range of decay rate constants is between 5×10^6 and 5×10^3 s^{-1}. It is interesting to see that in this way decay rates have been measured over a range of four orders of magnitude. The other experimental values were obtained by Klippenstein et al. [8] who measured $k(E)$ rates down to 4.48 eV using an ICR mass spectrometer. They agree quite well with our previous results between 4.5 eV and 4.8 eV if we correct them for IR relaxation.

For the perdeuterio benzene cation three decay rate values at large internal energies between ca. 5.3 eV and 5.5 eV were measured in our group, earlier. But no measurements at small internal energies have been performed so far. In this work we add a new value for perdeuterio benzene measured with an ICR mass spectrometer and the newly developed CIT-RETOF mass spectrometer.

In Fig. 9 all available experimental data is displayed. The values marked with filled circles are the ones originating from previous experiments of our group [5,26]. Now, IR relaxation is included in the evaluation of the decay rates by subtraction of a radiative decay rate of 700 s^{-1} from the measured decay rates between 4.6 and 4.8 eV in order to achieve the dissociation decay rate $k_{tot}(E)$. The open circles in Fig. 9 are those which were obtained by Klippenstein et al. taking into account the IR relaxation. The new value of 1150 s^{-1} of this work obtained for the decay rate of the perdeuterio benzene cation at a lower internal energy of 4.64 eV is marked with a filled triangle. The necessary IR relaxation correction (350 s^{-1}) for this value is nearly 25% of the measured rate value. This demonstrates the difficulty to obtain reliable decay rates in the ms time range where the internal energy of hot ground state ions is no longer simply related to the energy of the exciting photon.

It is interesting that the decay rate of the perdeuterio benzene cation is smaller by a factor of 10 than that of the benzene cation. This demonstrates the large intermolecular kinetic isotope effect for the H,D ejection at low excess energies which is expected for a statistical decay from the RRKM theory due to the different density of states in the activated complex close to the threshold [31,32]. The solid lines in Fig. 9 are the result of calculations according to the RRKM theory for the potential surface of the ground electronic $\tilde{X}(^2E_{1g})$ state. Assuming reasonable activated complexes the individual decay rates were calculated for the two C-loss channels and the two H-loss channels yielding the total rate constant as a sum of the individual decay rate constants. Experimentally found isotope effects in the high energy range ($E > 5.0$ eV) have been taken into account and reproduced by a suitable choice of reaction coordinates and frequencies of the activated complex. This leads to a smaller number of adjustable parameters because the Redlich-Teller product rule (see Ref. [32] p. 348). In this way, the curve for perdeuterio benzene was extrapolated down to ca. 4.5 eV although only three experimental values are available around 5.4 eV internal energy. In order to consider the IR relaxation correction of our four smallest decay rate values for the benzene cation and the new experimental value for the perdeuterio benzene cation mainly the frequencies of the activated complex for the C_2D_2 and C_3D_3 loss channel had to be slightly reduced. Only the values measured in our laboratory are included in the fitting procedure of the RRKM curve. In Tables 1 and 2 the vibrational frequencies of the assumed activated complexes of all four decay channels of benzene and perdeuterio benzene are given. For definition of the activated complex, see also previous work [5]. The threshold energies for the perdeuterio benzene decay channels are given by the threshold energies of the benzene decay channels and the difference of the zero point energy in the calculation. All threshold energies of this work differ only slightly from the respective values of our previous work but there is a trend towards larger threshold energies as suggested by Klippenstein et al. in their theoretical treatment performed at a higher level [8].

5. Summary and conclusion

In this contribution we presented new decay rates measured for the unimolecular dissociation of the benzene cation, which has been a prototype system for the investigation of a statistical unimolecular decay. The internal energy selection of the benzene cation was achieved by multiphoton excitation with ns laser pulses and checked by time-of-flight photoelectron and mass analyzed pulsed field threshold ionization (MATI) spectroscopy. We compared the decay rates obtained with to different ion storage devices by measuring the appearance of $C_6D_5^+$ cations from a decay of the perdeuterio benzene cation. The difference found is within the experimental uncertainty. The first device is a commercial Fourier-transform ion

Table 1
Threshold energies E_0, reaction pathway degeneracy and vibrational frequencies used for the calculation of the total decay rate $k_{tot}(E)$ of the benzene cation (taken from [33])

	Activated complex			
	H-loss	H_2-loss	C_2H_2-loss	C_3H_3-loss
	E_0 = 3.66 eV	3.74 eV	4.13 eV	4.19 eV
Educt	6	6	12	12
976	976	976	3315	3015
3130	3130	3130	3133	3033
1246	1246	1246	3133	3033
415	415	415	3060	3080
745	745	745	2731	2831
673	673	673	2731	2831
355	355	355	430	850
3077	3077	3077	370	966
3077	1516	1516	665	555
1516	1516	1516	1788	1788
1516	520	1250	2000	2121
1148	520	1250	1435	1435
1148	581	581	1341	1341
581	581	581	1288	1308
581	518	518	1288	1308
518	936	936	1190	1190
936	3159	3159	1097	1087
3159	1570	1700	1097	1087
1570	1148	1148	919	910
1148	314	314	878	878
314	314	314	696	694
314	718	718	651	651
718	718	718	637	672
718	919	919	160	120
919	919	919	283	283
919	1330	1330	268	268
1330	1330	1330	216	113
1330	3082	3082	125	113
3082	3082	3082	125	219
3082				

Table 2
Threshold energies E_0, reaction pathway degeneracy and vibrational frequencies used for the calculation of the total decay rate $k_{tot}(E)$ of the perdeuterio benzene cation (similar to [33])

	Activated complex			
	D-loss	D_2-loss	C_2D_2-loss	C_3D_3-loss
	E_0 = 3.74 eV	3.80 eV	4.19 eV	4.22 eV
Educt	6	6	12	12
927	927	927	2530	2320
2120	2120	2120	2351	2243
967	957	957	2351	2423
351	341	341	2260	2260
604	604	604	2080	2125
637	637	637	2180	2125
343	333	333	419	819
2300	2200	2200	352	920
2300	1390	1390	633	528
1390	1390	1390	1703	1703
1390	310	887	1904	2020
819	310	887	1151	1051
819	410	410	992	992
410	410	410	968	969
410	372	372	968	969
382	864	864	882	882
884	2360	2360	824	824
2370	1544	1750	824	824
1564	805	815	693	667
815	268	268	643	643
278	268	268	532	530
278	560	560	477	477
590	560	560	467	508
590	742	742	153	111
752	742	742	271	269
752	1209	1209	255	256
1209	1209	1209	207	109
1209	2257	2257	124	109
2287	2257	2257	124	217
2287				

cyclotron resonance mass spectrometer (FTICR-MS) and the second one is a home built electrodynamical cylindrical ion trap incorporated in a home made reflectron time-of-flight mass spectrometer (CIT-RETOF MS). This demonstrates that reliable collision-free decay rate measurements in the ms range can be performed in a relatively simple and low cost ion trap. The measured decay rate is corrected for infrared relaxation. We performed RRKM calculations to fit this value and previous results from our group and found slightly increased dissociation thresholds for the H and D elimination. In conclusion, we presented a new value for the dissociation rate constant of perdeuterio benzene at a low internal energy. The complete set of decay rate constants of the two cationic benzenes, $C_6H_6^+$ and $C_6D_6^+$, between 10^3 and 2×10^6 s^{-1} now provide a more extended basis for higher level theoretical modeling of the unimolecular decay of the benzene cation.

Acknowledegments

The authors want to thank M. Koch for his assistance during the experiments at the CIT-

RETOF mass spectrometer and Ch. Berg, Th. Schindler and G. Niedner-Schatteburg for their support running the FTICR instrument. Financial support from the Deutsche Forschungsgemeinschaft and the Fonds der Chemischen Industrie is gratefully acknowledged.

References

[1] B. Andlauer, C. Ottinger, Z. Naturforsch., A 27 (1972) 293.
[2] H.M. Rosenstock, J.T. Larkins, J.A. Walker, Int. J. Mass. Spectrom. Ion Phys. 11 (1973) 309.
[3] T. Baer, G.D. Willett, D. Smith, J.S. Phillips, J. Chem. Phys. 70 (1979) 4076.
[4] H. Kühlewind, H.J. Neusser, E.W. Schlag, J. Phys. Chem. 88 (1984) 6104.
[5] H. Kühlewind, A. Kiermeier, H.J. Neusser, J. Chem. Phys. 85 (1986) 4427.
[6] A.L. Sobolewski, C. Woywod, W. Domcke, J. Chem. Phys. 98 (1993) 5627.
[7] O. Braitbart, E. Castellucci, G. Dujardin, S. Leach, J. Phys. Chem. 87 (1983) 4799.
[8] S.J. Klippenstein, J.D. Faulk, R.C. Dunbar, J. Chem. Phys. 98 (1993) 243.
[9] R.C. Dunbar, in L.M. Babcock, N.G. Adams (Eds.), Advances in Chemistry, JAI, Greenwich, CT, 1996, Vol. 2, p. 87.
[10] P. Caravatti, M. Allemann, Org. Mass Spectrom. 26 (1990) 514.
[11] Ch. Berg, Th. Schindler, G. Niedner-Schatteburg, V. Bondybey, J. Chem. Phys. 102 (1995) 4870.
[12] Th.L. Grebner, H.J. Neusser, Int. J. Mass Spectrom. Ion Processes 137 (1994) L1.
[13] M. Benilan, C. Audoin, Int. J. Mass Spectrom. Ion Phys. 11 (1973) 421.
[14] B.A. Mamyrin, V.I. Karataev, D.V. Shmikk, V.A. Zagulin, Sov. Phys. JETP 37 (1973) 45.
[15] R. Weinkauf, K. Walter, C. Weickhardt, U. Boesl, E.W. Schlag, Z. Naturforsch., A 44 (1989) 1219.
[16] J.A. Booze, M. Schweinsberger, Tomas Baer, J. Chem. Phys. 99 (1993) 4441.
[17] U. Boesl, H.J. Neusser, E.W. Schlag, Z. Naturforsch., A 33 (1978) 1546.
[18] L. Zandee, R.B. Bernstein, D.A. Lichtin, J. Chem. Phys. 69 (1978) 3247.
[19] H.J. Neusser, Int. J. Mass Spectrom. Ion Processes 79 (1987) 141.
[20] S.R. Long, J.T. Meek, J.P. Reilly, J. Chem. Phys. 79 (1983) 3206.
[21] H. Kühlewind, A. Kiermeier, H.J. Neusser, E.W. Schlag, in G.S. Hurst, C.G. Morgan (Eds.), Resonance Ionization Spectroscopy, Institute of Physics, Bristol, England, 1986, p. 121.
[22] L. Zhu, P.M. Johnson, J. Chem. Phys. 94 (1991) 5769.
[23] H. Krause, H.J. Neusser, J. Chem. Phys. 97 (1992) 5923.
[24] H. Krause, H.J. Neusser, J. Photochem. Photobiol. A 80 (1994) 73.
[25] A. Kiermeier, H. Kühlewind, H.J. Neusser, E.W. Schlag, S.H. Lin, J. Chem. Phys. 88 (1988) 6182.
[26] H.J. Neusser, J. Phys. Chem. 93 (1989) 3897.
[27] M.S. Ahmed, H.Y. So, R.C. Dunbar, Chem. Phys. Lett. 151 (1988) 128.
[28] R.C. Dunbar, J. Chem. Phys. 90 (1989) 7369.
[29] R.C. Dunbar, Mass Spec. Rev. 11 (1992) 309.
[30] D. Stöckigt, J. Hrusak, H. Schwarz, Int. J. Mass Spectrom. Ion Processes 149 (1995) 1.
[31] R.A. Marcus, O.K. Rice, J. Phys. Colloid. Chem. 55 (1951) 894.
[32] W. Forst, Theory of Unimolecular Reactions, Academic, New York, 1973.
[33] A. Kiermeier, Ph.D. thesis, Fachbereich für Chemie, Biologie und Geowissenschaften der Technischen Universität München, 1988.
[34] H. Krause, Ph.D. thesis, Fachbereich für Chemie, Biologie und Geowissenschaften der Technischen Universität München, 1993.